IDENTIFICATION AND QUANTIFICATION OF NONSTATIONARY CHAOTIC BEHAVIOR

Ted W. Frison
Randle, Inc.
P.O. Box 1010
Great Falls, VA 22066
ted@chaotic.com
http://www.cquest.com/chaos.html

Henry D. I. Abarbanel
Institute for Nonlinear Science, Department of Physics and
Marine Physical Laboratory, Scripps Institution of Oceanography
University of California, San Diego
hdia@hamilton.ucsd.edu

ABSTRACT

Nonstationary chaotic behavior is not an oxymoron. We present two methods for capturing nonstationary chaos, then present a few examples including biological signals, ocean waves and traffic flow. The issue is of practical interest because it is often useful to capture when nonstationary events take place and it is desirable to know over what periods a signal is stationary.

INTRODUCTION

A signal is stationary if there is no change in the parameters of the underlying system. In the frequency domain, nonstationary behavior is often detected by comparing the power spectrum within windows to the power spectrum of the ensemble data. Because the Fourier coefficients describe the system in the frequency domain, any significant variation implies a change in parameters and the system is considered nonstationary.

Chaotic signals are inherently broad-band and present many difficulties for linear processing methods, not the least of which is that changes in behavior may take place that are not manifest in the Fourier spectrum. The broad-band nature of stationary chaotic signals can give them the illusion of being nonstationary. Using a parameter change in the well studied chaotic Lorenz system, we illustrate the point in figure 1 where the FFT after a parameter change is almost unchanged.

Fortuitously, phase space reconstruction[1,2] allows us to define a Euclidian space where a proxy for the full multivariate system can be created. Several robust metrics have been invented to classify chaotic signals[3]. We have modified one of these algorithms to operate within windows in a manner similar to windowed FFTs to capture parameter changes in chaotic systems. The basic method of false nearest neighbors is used to determine the embedding dimension (degrees-of-freedom) required to embed the entire attractor.

GLOBAL EMBEDDING DIMENSION

The minimum embedding dimension, d_E, is the degrees of freedom needed to describe the system over the entire data set. This is also the number of geometric dimensions that are needed to fully reconstruct the attractor.

The method of false nearest neighbors[4] relies on the geometric basis for the theorem of Mañè and Takens. If the dimension is too low, points are projected down into the lower dimension. As the dimension is increased, attractors "unfold." Points on trajectories that appear close in dimension d may move to a distant region of the attractor in dimension $d+1$. These are "false" neighbors in d and the method measures the percentage of false neighbors as d increases. Points that are close in d are tallied, and the number of these points that become widely separated in $d+1$ are

calculated.

The nearest neighbor to y(n) is $y^{NN}(n) = (v^{NN}(n), v^{NN}(N+T), \ldots, v^{NN}(n+(d-1)T))$. The neighbor is false in dimension *d* if

$$\left[\frac{R_{d+1}^2(n)}{R_d^2(n)}\right] = \frac{|v(n+Td) - v^{(r)}(n+Td)|}{R_d(n)} > R_{tol1}$$

where $R_d(n)$ is the Euclidian distance between a point y(n) and its nearest neighbor $y^{NN}(n)$ and R_{tol} is the criteria for declaring whether the neighbors that are close in d are distant in d+1.

A second criterion is necessary because the nearest neighbor may not necessarily be "close." The density of the vectors in space may be low as the dimension increases. That is, as dimensions are added the proportionate volume occupied by the signal will decrease and the distance to neighbors will increase. If the nearest neighbor to a point is false but not close, then the Euclidian distance in going to d+1 will be ~ $2R_A$. So, the second criteria is

$$\frac{R_{d+1}(n)}{R_A} > R_{tol2}$$

where R_A is the mean size of the attractor. A nearest neighbor is false if either test fails.

For a noiseless signal, the number of false neighbors becomes zero when the minimum embedding dimension d_E is reached. A noisy signal drops off dramatically, but never reaches zero. For SNRs as low as 6 to 10 dB, the percentage of false neighbors drops below 1% for $d \geq d_E$. The advantage of this technique is that it is relatively robust to noise and data corruption. Even is relatively high noise cases, it will yield valid results when other methods fail[3,4]. Experience has also shown that false nearest neighbor testing will work for short data sets. That is, we can apply it to short time series and get valid results, a fact that we will use shortly.

Thus, we can use the change in the percentage of false neighbors as a clue that a parameter change has taken place. For the Lorenz system, the points where the parameter changes take place is noticeable (x axis), Figure 2 (the vertical axis is the percentage of false neighbors). Each line is a trial dimension (*d*). In these calculations, the embedding dimension at any point is derived from the cross section of Figure 2 and remains constant across the nonstationary events, despite the change in the relative number of false neighbors. Figure 2 also gives some clues as to why many gross metrics of chaotic behavior, such as fractal dimension proxies, fail to properly identify pathological events in real data -- parameter changes can take place without a change in dimension.

As a practical example, Figure 3 shows Hurricane Camille as it overran an oil platform in the Gulf of Mexico. The nature of the storm remains relatively unchanged until window 300 (sample 75,000) when the worst part of the storm hit the platform. Figure 4 shows traffic flow counts on a freeway outside Houston, Texas, USA. Although the indication is subtle, a traffic jam slowly builds starting at sample 100 (this is really a time index).

LYAPUNOV EXPONENTS

The Lyapunov exponents describe the rate at which close trajectories diverge. If one or more Lyapunov exponents is positive, the trajectories diverge, the system is unstable, and the underlying system is chaotic[5].

The Lyapunov exponents may be computed from the signal by a recursive QR decomposition technique [6] from the Jacobian of a function, F[y(n)], that maps points on the orbit into points at the t time steps later, y(n+t) = F[y(n)]. Typically, we do not know the map and must estimate the Jacobian matrix of this dynamical rule using state space and temporal knowledge of the orbit points y(n).

The map describes nearby orbits and how the distance between these neighbors change over time. The distance between the orbit and the r^{th} neighbor at T_0 is $z^r(n;0)$. The corresponding distance at a time t later is: $z^r(n;t) = F[y(n) + z^r(n;0)] - F[y(n)]$.

A Taylor series expansion of F[•] contains the Jacobian of the underlying dynamics as the first term of this expression. The terms in the often ill-conditioned Jacobian matrix are found by a least squares minimization of the residuals in this formula.

The local Lyapunov exponents $\lambda_i(x,L)$; i

= 1,2,...,d are the eigenvalues $e^{[L\lambda_i(x,L)]}$ of the Oseledec matrix, $\boldsymbol{OSL}(x,L) = [(\boldsymbol{DF}^L(x))^T \bullet \boldsymbol{DF}^L(x)]^{1/2L}$ where $\boldsymbol{DF}^L(x)$ is the product of L Jacobian matrices $\boldsymbol{DF}(x)$. The $\lambda_i(x,L)$ become independent of x as $L \rightarrow \infty$ by the multiplicative ergodic theorem[20]. These are the global Lyapunov exponents. For finite L, the local Lyapunov exponents, which vary widely over the attractor, measure the growth rate of perturbations for L samples. The local dimension, d_L, is determined by computing distances in d_E, but making local fits for $\boldsymbol{DF}(x)$ in $d_L \leq d_E$ [7].

This method is notable because the Lyapunov exponents can be calculated directly from the data and works remarkably well on short series. The primary consideration is performing the calculations over enough starting locations to achieve a good estimate.

In aggregate, the Lyapunov exponents are useful mainly for classification of chaos and deriving an estimate of the horizon over which one can have confidence in predictions of future state [8].

Because the Lyapunov exponents vary over the attractor (that is, they vary with time), tracking the evolution of the largest exponent (at the limit L) provides clues as to the stability of the underlying system as it evolves.

Using a method similar to that described above, we track the change in the largest Lyapunov exponent in data from a biological system that is suddenly placed under stress, Figure 5. In this case, the system comes to rest until the stressing event starts at about 500 seconds. The event continues until 600 seconds (the vertical bar). The largest Lyapunov exponent increases rapidly during this event, then fluctuates but holds the higher level for some time, then begins a descent back toward some new steady state region. The nonstationary event is clearly identified by the change in the exponent.

For this example, 25,000 samples were used to form the attractor and the estimate of the exponent was based on 2,000 starting locations inside the window. For each point, the window was moved 500 samples.

In this case, the evolution of the largest Lyapunov exponent follows intuition about chaos in biological systems. The increase in the exponent might be expected for a "normal" system because chaotic systems are robust.

In general, we find the method of the windowed Lyapunov exponents provides better results because they are more sensitive to changes that occur within a given embedding dimension.

REFERENCES

[1] Mañè R., "On the Dimension of the Compact Invariant Sets of Certain Nonlinear Maps," in *Dynamical Systems and Turbulence, Warwick 1980,* eds. D. Rand and L.S. Young, *Lecture Notes in Mathematics* **898**, 230-242, (Springer, Berlin, 1981).

[2] Takens, F. "Detecting Strange Attractors in Turbulence," in *Dynamical Systems and Turbulence, Warwick 1980,* eds. D. Rand and L.S. Young, *Lecture Notes in Mathematics* **898**, 366, (Springer, Berlin, 1981).

[3] Abarbanel, Henry D. I., Analysis of Observed Chaotic Data, Springer Verlag (New York), 1996.

[4] Kennel, Matthew B., R. Brown, and H. D. I. Abarbanel, "Determining embedding dimension for phase-space reconstruction using a geometrical construction," *Phy. Rev. A* **45** pp. 3403-3411, 15 March 1992.

[5] Ruelle, D., Proc R. Soc. A **427** (1990) 241.

[6] Eckmann, J.P., S.O. Kamphorst, D. Ruelle, and S. Ciliberto, *Phys. Rev.* **A34**, 4971 (1986).

[7] Abarbanel, Henry D. I., *Analysis of Observed Chaotic Data*, Springer Verlag (New York), 1996.

[8] Frison, Theodore W., and Henry D. I. Abarbanel, "Ocean gravity waves: A nonlinear analysis of observations," in press, Jour. Geophysical Review-Oceans.

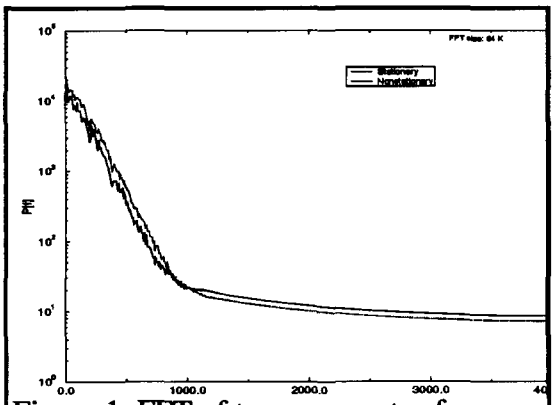

Figure 1. FFT of two segments of a nonstationary chaotic signal.

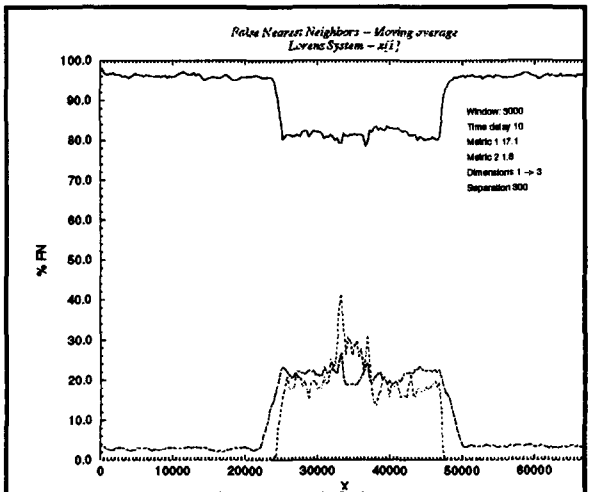

Figure 2. The windowed false nearest neighbor across the same data. Note change in the percentage of false neighbors at the nonstationary transitions while the embedding dimension remains constant.

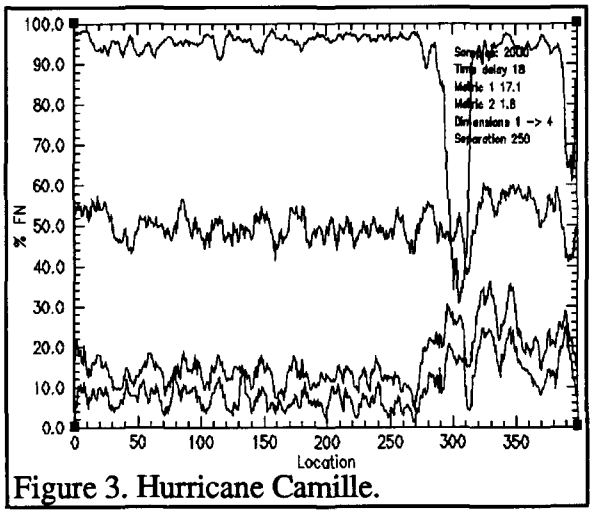

Figure 3. Hurricane Camille.

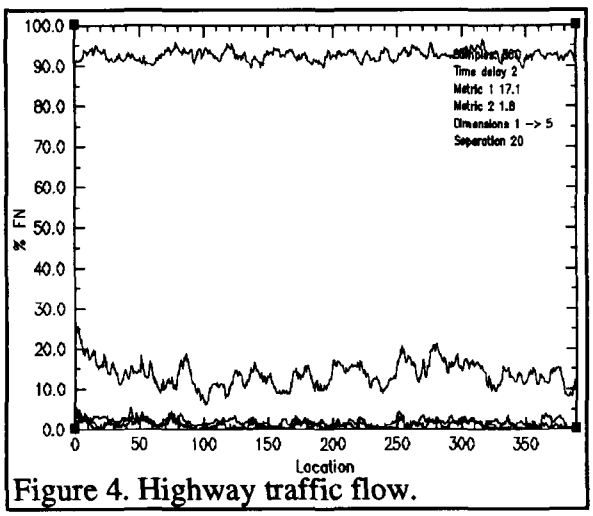

Figure 4. Highway traffic flow.

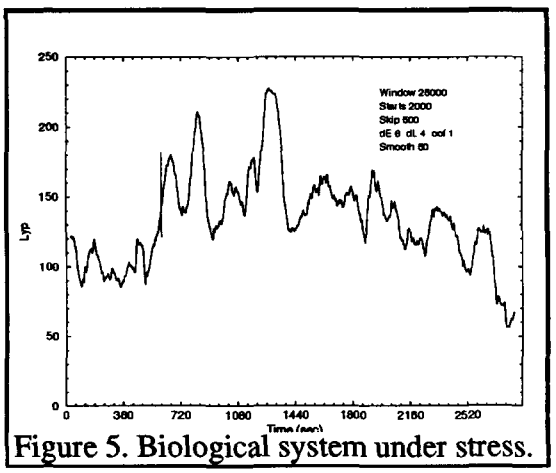

Figure 5. Biological system under stress.